pH-Dependent Electron-Transport Properties of Carbon Nanotubes

Ju Hee Back and Moonsub Shim*

Department of Materials Science and Engineering and Frederick Seitz Materials Research Laboratory, University of Illinois at Urbana-Champaign, Urbana, Illinois 61801

Received: May 26, 2006; In Final Form: September 11, 2006

Carbon nanotube electrochemical transistors integrated with microfluidic channels are utilized to examine the effects of aqueous electrolyte solutions on the electron-transport properties of single isolated carbon nanotubes. In particular, pH and concentration of supporting inert electrolytes are examined. A systematic threshold voltage shift with pH is observed while the transconductance and subthreshold swing remain independent of pH and concentration. Decreasing pH leads to a negative shift of the threshold voltage, indicating that protonation does not lead to hole doping. Changing the type of contact metal does not alter the observed pH response. The pH-dependent charging of SiO_2 substrate is ruled out as the origin based on measurements with suspended nanotube transistors. Increasing the ionic strength leads to reduced pH response. Contributions from possible surface chargeable chemical groups are considered.

Introduction

A combination of exceptional electrical and mechanical properties of carbon nanotubes[1] is prompting numerous research directions and technological innovations from nano-electromechanical systems[2] and flexible macroelectronics[3] to miniaturized biosensors[4] and novel composite materials.[5] In the ideal limit, a single-walled carbon nanotube (SWNT) may be considered as a rolled up graphene sheet leading to a seamless cylinder without any surface dangling bonds. SWNTs are often considered as prototypical one-dimensional conductors and semiconductors with current densities reaching $10^9 A/cm^2$ and carrier mobilities on the order of 100000 $cm^2/V \cdot s$.[6] In addition, having all atoms at the surface leads to highly exposed electronic wave functions which in turn provide extremely sensitive properties. Combined with completely satisfied surface bonds in the ideal limit (which would provide chemical inertness), utilizing SWNTs as a robust medium to convert and to amplify one or a small number of molecular events into easily detectable electrical or optical signals may be envisioned.[7]

However, highly sensitive electronic properties of SWNTs have led to many difficulties and debates over their intrinsic properties. For example, whether charge-transfer interaction upon adsorption of oxygen from the ambient occurs or not still remains an open debate.[8] Pronounced response of SWNTs to pH change and therefore presumably to protonation has been interpreted in several different ways. When SWNTs are dispersed in or exposed to neat superacids[9] or concentrated H_2SO_4,[10] direct protonation leading to $C{:}H^+$ moiety has been shown. In milder conditions, optical bleach of the band edge transitions has been observed at low pHs in laser ablation SWNTs rendered water-soluble by strong acid treatment.[11] This optical bleach has been attributed to protonation of covalent carboxylate groups on the side walls of SWNTs.[11] In sodium dodecyl sulfate (SDS) dispersed SWNTs synthesized by a high-pressure CO method, similar optical bleach upon lowering of solution pH has been suggested to arise from sidewall protonation, leading to electron localization but not necessarily via processing-induced carboxylate groups.[12] In these SDS-dispersed tubes, pre-adsorbed O_2 has been suggested to mediate the reversible protonation process with metallic tubes having the highest affinity toward protons.[13] In semiconducting tubes, proton affinity has been suggested to be band gap-dependent with smaller band gap SWNTs being protonated first.[13] Photoluminescence studies on the same system carried out by Weismen et al. have led to the conclusion that the observed pH-dependent optical properties of semiconducting tubes are diameter-dependent, rather than band gap-dependent.[14] Dukovic et al. have later suggested that these optical responses of SWNTs in relatively mild pH ranges are mediated by singlet O_2 adsorbed on SWNTs in the form of 1,4-endoperoxides. At pH $\sim$ 5 and below, these endoperoxide groups on the SWNTs are presumably protonated, leading to hydroperoxide surface moieties and positive charges in the tube (i.e., hole-doping).[15] While direct experimental proof of such a mechanism explaining the pH response of SWNTs remains a challenge to be demonstrated, these observations have important consequences on many fundamental aspects of SWNTs including the actual surface chemical composition in ambient conditions, chemical reactivity, and the effects of the local chemical environment on the extended π-electronic structure arising from all-surface C atoms. To help elucidate the surface composition and chemistry of SWNTs, we report on the electrical responses of isolated individual SWNTs in electrochemical transistors[16] to pH and electrolyte concentration under inert KCl electrolyte solution. These studies should in turn provide some of the necessary understanding, especially with respect to the effects on the electron-transport characteristics, for developing SWNT-based technologies, many of which require well-defined surface functionalization.

Experimental Section

Individual SWNT transistors were fabricated by catalyst-assisted chemical vapor deposition (CVD) synthesis reported previously.[17] Briefly, catalyst containing $Fe(NO_3)_3 \cdot 9H_2O$ and alumina or ferritin (Sigma) diluted 1000 times with deionized

* To whom correspondence should be addressed. E-mail: mshim@uiuc.edu.

10.1021/jp063260x CCC: $33.50
Published on Web 10/24/2006

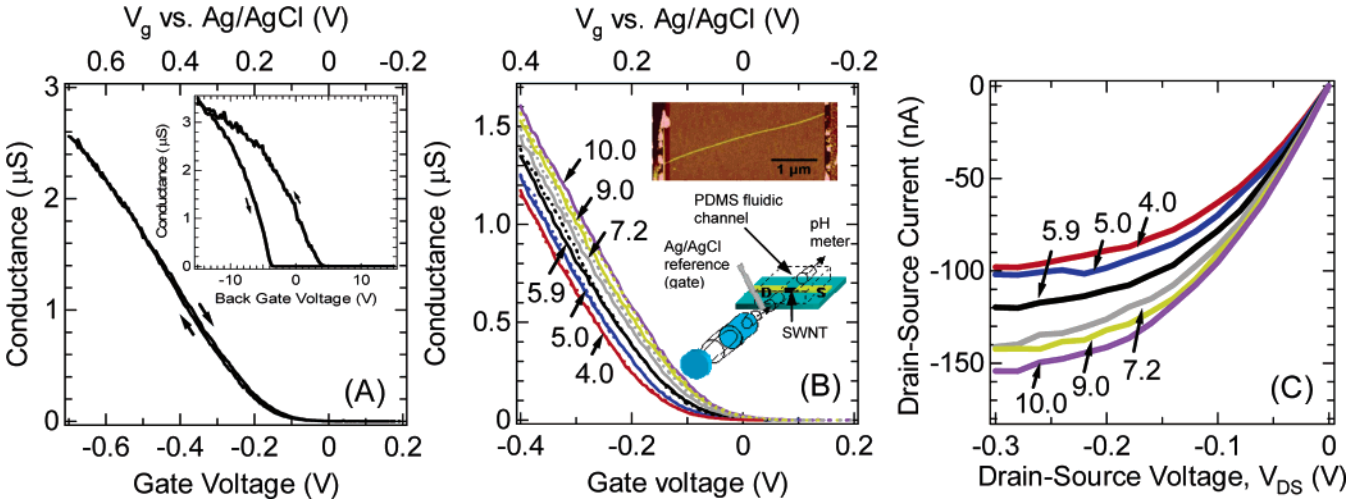

Figure 1. (A) Comparison of transfer characteristics of a single semiconducting tube operating with electrolyte gate and with back gate (inset). (B) Changes in the transfer characteristics of a semiconducting tube upon increasing (solid lines) and decreasing (dashed lines) pH. The numbers correspond to the pH of the solution. Upper inset is the AFM image of the device and the lower inset is the schematic of the device integrated with a microfluidic channel. (C) Output characteristics of the same semiconducting tube at $V_g = -0.3$ V with indicated pH. All electrolyte gate measurements are carried out with 10 mM KCl solution.

water was patterned by optical lithography on a Si/SiO_2 substrate. CVD growth was carried out with CH_4 and H_2 at 900 °C for 10 min. For electrical contacts, different metal sources, Ti/Au (~3/~30 nm), Ti/Au (~30/~30 nm), or Pd/Au (~30/~30 nm), were evaporated on top of SWNTs with 1−4 μm spacing between the source and the drain electrodes. For measurements addressing contact contributions, device annealing was carried out at 300 °C under Ar flow for 10 min or immersed in 1 mM hexadecanethiol (Aldrich) in ethanol for 1 day to create a monolayer of thiols on Au as indicated. Suspended SWNT devices were fabricated by etching away the substrate of 1 μm channel length devices with 10:1 buffered HF solution.

For electrolyte gating, a poly(dimethylsiloxane) fluidic channel was placed over the individual SWNT transistors and the device was allowed to equilibrate under deionized water for several hours prior to measurements. Then aqueous KCl solution was injected into the fluidic channel. The pH of electrolyte solution was adjusted by adding the appropriate amounts of HCl or KOH of the same ionic strength dropwise while monitoring with a pH meter. A leak-free Ag/AgCl reference microelectrode was used to apply the electrochemical gate voltage. For concentration dependence, measurements made with the Ag/AgCl microelectrode were compared to those made with Ag/AgCl double-junction reference electrode to ensure that the concentration gradient does not interfere with applied and measured potentials. The electrolyte solutions bubbled with Ar immediately prior to injection into the microfludic channel for measurements did not lead to any noticeable differences compared to solutions without Ar bubbling. Raman measurements were carried out on a Jobin Yvon LabRam HR 800 micro-Raman spectrometer with 633 nm (1.96 eV) excitation source with SWNTs grown on fused quartz substrates to allow measurements from the backside with a 100× air objective. All measurements were carried out in air at room temperature.

Results and Discussion

Especially due to significant diameter and chirality distributions in any given ensemble of SWNTs synthesized by currently available methods, measurements at the single nanotube level is particularly important in understanding basic physical and chemical properties of SWNTs.[18,19] In some cases, catalyst metal particles and possible amorphous residues can be present in larger quantities than nanotubes, leading to ensemble response that is dominated by side products.[20] In addition, effects of processing conditions[21] need to be carefully considered as surface functional groups whether intentional or not will inevitably modify chemical reactivity. By patterned growth of SWNTs using CVD methods, harsh processing conditions can be avoided and measurements can be carried out where metal catalysts and potential amorphous residues are not present. The pH-dependent electrical response of isolated single semiconducting SWNTs under 10 mM KCl solution is first discussed. We then discuss potential extrinsic factors (substrate and contacts) that may contribute to the observed behavior. For insights on the origin of the intrinsic SWNT pH response, supporting inert electrolyte concentration and diameter dependencies are then presented.

pH Response of Isolated Single Semiconducting Tubes. Figure 1a compares the transfer characteristics of a single SWNT transistor under 10 mM KCl solution with the same device operating with a back gate (inset). The large hysteresis in the back gate operation,[22] which presumably arises from electrons being trapped on the substrate, is completely removed under electrolyte gate operation. This difference may be attributed to the high gate efficiencies allowing small voltage operation and short Debye lengths screening potential charge traps. Figure 1b shows the transfer characteristics of an electrolyte-gated single SWNT transistor at the indicated pHs. The upper inset in Figure 1b is the AFM image of the device and the lower inset is the schematic of the device geometry. The pH of the solution is first varied from 4 to 10 (solid lines) and then back to 4 (dashed lines). There is a systematic negative shift in the threshold voltage with decreasing pH. Figure 1c shows the output characteristics at a fixed gate voltage ($V_g = -0.3$ V) for the indicated pH solutions consistent with the transfer characteristics. The negative shift in the threshold voltage without significant transconductance change indicates that lowering the pH of the solution is likely to lead to a decrease in the hole concentration in the tube. Note that unlike the back gate operation where the large hysteresis can complicate determination of threshold voltage, electrolyte gating using a reference electrode allows changes in the threshold voltages to be easily detected.

Figure 2 shows the radial breathing mode (A) and the G-band (B) regions of the Raman spectra of a semiconducting SWNT.

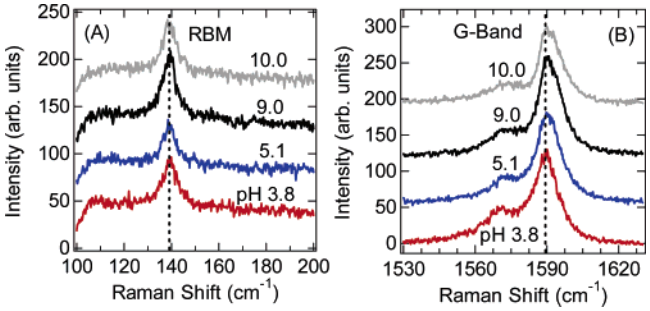

Figure 2. Radial breathing mode (A) and tangential G-band (B) regions of the Raman spectra of a single semiconducting SWNT under 10 mM KCl solution of indicated pH.

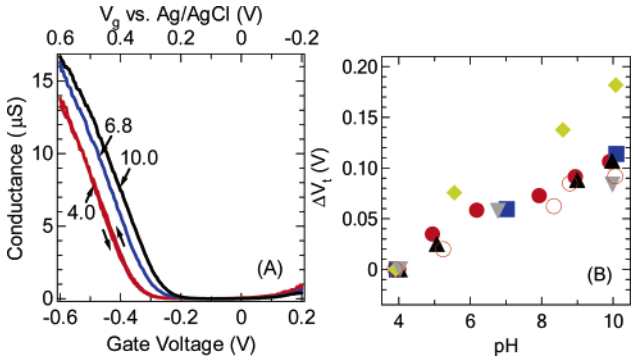

Figure 3. (A) Transfer characteristics of Pd-contacted semiconducting nanotube at the indicated pH (10 mM KCl). Both forward and reverse sweeps are shown for pH 4. (B) pH-dependent threshold voltage shift of individual SWNT transistors with various contacts: 3/30 nm thickness Ti/Au (●), Ar annealed 3/30 nm Ti/Au (■), hexadecanethiol monolayer on 3/30 nm Ti/Au (▲), 30/30 nm Pd/Au (▼), 30/30 nm Ti/Au (◆), and 30 nm Ti only (○).

There is no noticeable change in the frequency and the line width of the radial breathing mode from pH 4 to pH 10. Similarly, very little or no change with increasing pH is observed in the G-band region. A slight line broadening in the G-band region may be occurring at pH 4, which would be consistent with ensemble measurements in solution reported in ref 13. There is no detectable disorder mode around 1300 cm^{-1} for this SWNT (as well as other semiconducting tubes that we have examined) and changing the solution pH does not induce disorder mode as expected for noncovalent processes.

The absence of or insignificant Raman spectral changes may be explained by the magnitude of the threshold voltage shift observed in the electrical measurements. Since the change in the carrier density $\Delta Q = C_g \Delta V_t$, where C_g can be estimated to be the nanotube quantum capacitance of $\sim 4 \times 10^{-10}$ F/m due to the fact that the electrolyte gate capacitance is significantly larger,[16a] the negative threshold shift (ΔV_t) of ~100 mV from pH 10 to pH 4 shown in Figure 1b corresponds to a decrease in the carrier concentration of ~0.25 holes/nm or approximately 0.002 holes/C atom. If we assume that there is a linear relation between the G-band spectral shift and the carrier density change ($|\Delta\omega_G/\Delta Q|$ = constant < 600 cm^{-1}/carrier/C atom, based on reports of electrochemical/charge transfer doping[23]), then we expect a spectral upshift of about ~1 cm^{-1} or less for an increase in the hole density of ~0.002/C atom. This small, expected G-band shift is close to our spectral resolution. Based on the essentially complete band edge transition bleach reported,[13,15] a significant upshift in the tangential G-band is expected[23b] if protonation had led to hole injection in SWNTs. However, at the low doping fraction changes that we observe, the situation may be complicated by the fact that the linear relation between $\Delta\omega_G$ and ΔQ may not hold and other factors such as the anomalous spectral shifts as observed in alkali metal doping[24] may be taking place. What we observe is that there is an insignificant shift (or a slight downshift, if any) of the G-band features in Figure 2b *inconsistent* with the picture of hole injection via low pH-induced protonation.[15] Furthermore, our electrical measurements show significant negative threshold shifts of ~100 mV from high to low pH which means that if any carriers are injected they are electrons (or that the holes are removed).

While the above observations suggest that protonation under relatively mild conditions (pH > 2) does *not* lead to hole injection, other extrinsic factors such as the effects of the substrate which should also have pH-dependent properties (i.e., pH-dependent surface charge density) and contacts especially for electrical measurements need to be carefully considered before any conclusions can be made. Therefore, we discuss below the responses of SWNTs with different metal contacts as well as suspended SWNT transistors where the substrate is removed before considering a possible origin of the pH-dependent electrical response.

Effects of Metal Contacts. Depending on the choice of metal contacts, SWNT transistors are known to have varying operation mechanisms and performances.[1a,b,8a−d] In addition to the work function difference-induced variations in the Fermi level pinning, molecular adsorption can alter the nature of SWNT−metal contacts.[8a,b,d] We have shown previously that low-intensity UV-induced desorption of oxygen occurs from the native oxide layer of the Ti contacts modulating Schottky barriers whereas Pd-contacted SWNTs show essentially no UV response.[8a,b] Thermal desorption, on the other hand, can lead to changes directly on SWNTs consistent with doping changes.[8a] The SWNT devices discussed above have Au electrodes with ~3 nm Ti adhesion layer and protonation of Ti native oxide layer and/or other processes at the contacts may be responsible for the observed changes. To address the potential contribution from the metal contacts, various metals and insulating thiol monolayers have been examined. Figure 3a shows the transfer characteristics of a Pd-contacted SWNT transistor at the indicated pHs. In all cases, the supporting electrolyte concentration is 10 mM. The same behavior (negative threshold shift without significant changes in the transconductance with decreasing pH) as the Ti/Au electrodes is observed.

Figure 3b shows the shift of the threshold voltage with pH for individual SWNTs contacted with various metal electrodes. Whether the contact metal is only Ti, Au with different Ti adhesion layer thicknesses, Pd with Au capping layer, or Ti/Au insulated with hexadecanethiol monolayer, the overall response remains the same. In all cases, there is about 100 mV negative shift in the threshold voltage without a significant transconductance change from pH 10 to pH 4. Interestingly, more than a 4-fold increase in the on-state conductance by thermal annealing of Ti/Au contacted SWNT at 300 °C under Ar (which indicates a significant improvement in the electrical contacts) does not alter the qualitative pH response as well as the magnitude of the threshold voltage shift. Based on these observations, we conclude that SWNT−metal contact has little or no effect on the observed pH response of SWNT transistors.

Effects of Substrate. All SWNT transistors as well as electrically isolated SWNT samples for Raman measurements examined here are grown on Si/SiO_2 or fused silica substrates. Surface charge density of SiO_2 varies with pH with the isoelectric point usually between pH 2 and pH 4. Silica colloids prepared by the Stober method have been shown to exhibit

surface charge density change on the order of ~10 μC/cm^2 from pH 4 to pH 9 in 10 mM KCl.[25] This change in surface charge density should, in principle, contribute to the double-layer capacitance for electrochemical gating. Assuming a uniform charge distribution, a constant offset in the gate potential would arise due to a fixed surface charge density σ. For simplicity, we estimate this surface charge contribution to be the potential drop from the surface to the Debye length away from the surface. For our 1:1 electrolyte KCl, the surface potential is given by the Grahame equation as

$$\phi_s = \frac{2kT}{e}\sinh^{-1}\left(\frac{\sigma}{\sqrt{8\epsilon\epsilon_o kTC_o}}\right) \quad (1)$$

and the potential at Debye length away from the surface can be obtained from Guoy-Chapman theory as

$$\phi_D = \frac{2kT}{e}\ln\left(\frac{1+\gamma}{1-\gamma}\right) \quad (2)$$

Here kT is the thermal energy, e is the electric charge, ϵ is the dielectric constant of the solution around the nanotube, ϵ_o is the vacuum permittivity, C_o is the bulk electrolyte concentration, and $\gamma = e^{-1}\tanh(e\phi_s/4kT)$. We estimate the offset in the electrochemical gate potential as $\Delta\phi \approx \phi_D - \phi_s$ and the threshold voltage shift between two different pH values of pH_a and pH_b as

$$\Delta V_t \approx \Delta\phi(pH_a) - \Delta\phi(pH_b) \quad (3)$$

With use of σ (pH = 4) ~ 0 C/m^2 and σ (pH = 9) ~ −0.13 C/m^2 from ref 25 for 10 mM KCl solution (which is the same concentration as our measurement conditions) and the assumption that $\epsilon = 80$, the threshold voltage shift expected from pH 4 to pH 9 is $\Delta V_t \approx \Delta\phi(pH = 9) - \Delta\phi(pH = 4) \sim 100$ mV. While this estimate is very similar to the threshold voltage shift observed in Figures 1 and 3 and the correct direction of the shift is predicted (i.e., high pHs leading to more positive threshold voltage), caution must be taken since there may be other factors such as chargeable chemical groups on SWNT sidewalls that may have a more pronounced effect on the device characteristics.

To examine the influence of the substrate surface charges more directly, pH responses of SWNT transistors before and after etching away the SiO_2 substrate have been examined. Figure 4 shows the transfer characteristics of a SWNT transistor at different pHs after substrate etching via HF. Figure 4 upper inset compares the threshold voltage shift before and after the removal of the substrate. The lower inset is the SEM image of the device obtained after all measurements have been carried out, indicating that the SWNT is indeed suspended without capillary forces pulling the nanotube to the bottom of the etched trench. While there is a slight offset for a fixed pH, there is no significant differences in the magnitude and the direction of the threshold voltage shift from pH = 4 to pH = 10 for suspended and on-substrate SWNT transistors. Eight suspended SWNT transistors that we have examined all exhibit similar pH responses of ~100−200 mV negative threshold voltage shift with decreasing pH, strongly suggesting that the observed pH response of SWNT transistors is *not* likely to arise from substrate charging effects.

Supporting Electrolyte Concentration Effect. With the effects of the substrate and the SWNT−metal contacts ruled out as the potential origin of the pH response observed, we now discuss how pH-dependent electron-transport properties of

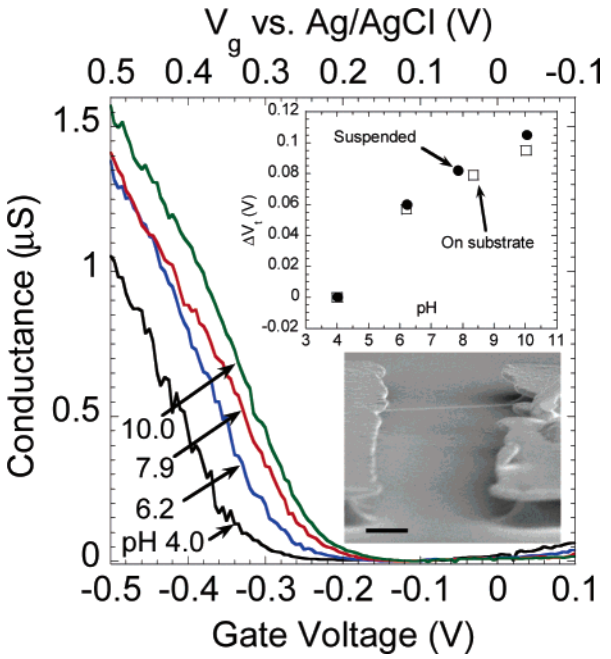

Figure 4. Transfer characteristics of a suspended SWNT transistor at the indicated pH (10 nM KCl). The top inset is the comparison of the pH-dependent threshold voltage shift before and after substrate etching. The lower inset is the SEM image of the device obtained after all measurements have been carried out confirming that the SWNT is suspended. The scale bar is 500 nm.

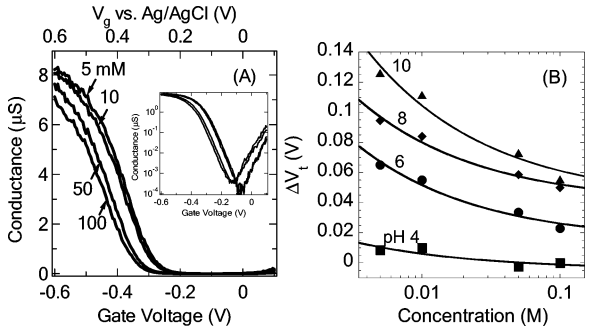

Figure 5. (A) KCl concentration-induced changes in the transfer characteristics of a SWNT transistor at pH 10. The inset shows the same plot in log scale for the conductance. There is no noticeable change in the subthreshold swing from 5 to 100 mM KCl concentration. (B) Concentration-dependent threshold voltage shift at the indicated pHs. All voltage shifts are measured with respect to the threshold voltage at 100 mM at pH 4. The lines are guides to the eye.

semiconducting SWNTs are affected by supporting electrolyte concentration. Figure 5a shows the transfer characteristics of a SWNT transistor at the indicated KCl concentration. In all cases, the solution pH is maintained at 10. There is a distinct shift of the transfer curves to a more positive gate voltage with decreasing concentration without noticeable change in the transconductance. Figure 5b shows the threshold voltage shift vs KCl concentration at the indicated pHs. The concentration dependence of the threshold voltage shift nearly disappears at the lowest pH of 4 and the magnitude of the threshold voltage shift with concentration increases with increasing pH.

Since we have used an inert salt as the supporting electrolyte in all cases, the main effect of the changes in the ionic strength of the solution should be the changes in the Debye length. An immediate consequence of the increase in the Debye length is the decrease in the electrochemical gate capacitance. For our measurements, a concentration range from 5 mM to 100 mM is examined which corresponds to Debye lengths from 4 to 1

nm, respectively. The electrochemical gate capacitance can be estimated as $C_{eg} \sim 2\pi\epsilon\epsilon_o/\ln(1 + 2\lambda/d)$, where λ is the Debye length and d is the nanotube diameter.[16a] The change in λ from 4 to 1 nm leads to an increase in C_{eg} from 2×10^{-9} to 4×10^{-9} F/m using $\epsilon = 80$ and $d = 1$ nm. Even the smallest capacitance is still 5 times larger than the nanotube quantum capacitance and therefore we do not expect a factor of 4 increase in the Debye length to play a significant role in the overall gate capacitance which should in principle be limited by the nanotube quantum capacitance. If we consider the dielectric constant within the Debye length from the nanotube surface to be about an order of magnitude smaller than that in the bulk H_2O as pointed out by Shimotani et al.,[26] then C_{eg} becomes comparable to the nanotube quantum capacitance. In this scenario, the gate efficiency would decrease with increasing Debye length which should appear as an increase the subthreshold swing and a decrease in the transconductance with decreasing KCl concentration. We do not observe any noticeable transconductance or subthreshold swing change with decreasing KCl concentration for the SWNT shown in Figure 5a.

At high pH, there is a significant concentration dependence of the threshold voltage shift as shown in Figure 5b. At low pH, the concentration dependence essentially disappears. One possible scenario that is consistent with these observations is if there were surface charges on SWNTs that become protonated at low pHs. For example, carboxylate or other oxygen-based sidewall chemical groups may provide the sources of such surface charges on SWNTs. If we consider chemical groups to be present on the SWNT surfaces, then there is a significant surface charge density at high pHs, leading to a similar effect as what we have considered above for substrate charge induced potential offset to the applied electrochemical gate potential. The quenching of the surface charges by protonation at low pH levels removes this electrochemical potential offset. At high ionic strengths, these surface charge-induced effects get screened out.

On the Origin of pH-Dependent Electrical Response. With the supporting electrolyte concentration dependence revealing that the electrical response of semiconducting SWNTs is consistent with possible surface charges, we now return to the pH-dependent threshold voltage shift at a fixed KCl concentration. We can estimate the potential offset to the electrochemical gate due to surface charges on SWNT surface utilizing eqs 1−3. If we assume that only protonation leads to quenching of the surface charges, then the surface charge density σ is related to the number of chargeable groups per unit area e/A and surface coverage θ by $\sigma = -e(1 - \theta)/A$. We take the Langmuir-Freundlich adsorption isotherm for θ to take into account that there may be a distribution of proton adsorption energies for different surface sites. Then the surface charge density is given by

$$\sigma = -\frac{e}{A}\left(1 - \frac{a[H^+]^m}{1 + a[H^+]^m}\right) \qquad (4)$$

where a is related to the average proton adsorption constant $K = a^{1/m}$ and m indicates the degree of heterogeneity of the binding sites.[27] Substituting eq 4 into the potentials at the surface and at Debye length given in eqs 1 and 2, respectively, then substituting the potentials into eq 3 gives the threshold voltage offset due to pH and the supporting electrolyte concentration changes. Figure 6 shows the pH-dependent threshold voltage shift for a single semiconducting nanotube measured at KCl concentration of 10 mM. The curve is calculated using $e/A =$ 0.08 C/m^2, proton adsorption constant $K = 5 \times 10^7$ (or $pK_a \sim 7.6$), and $m = 0.3$ and assuming that $\sigma \rightarrow 0$ at low pHs.

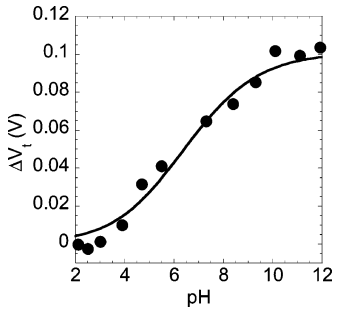

Figure 6. pH-dependent threshold voltage shift of a semiconducting SWNT transistor under 10 mM KCl solution. Solid circles are experimentally measured data points and the curve is calculated based on the model described in the text.

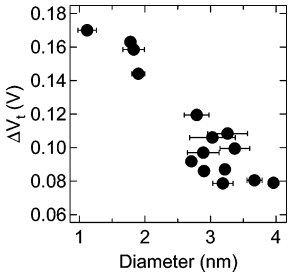

Figure 7. Dependence of threshold voltage shift [$\Delta V_t = V_t$ (pH = 10) − V_t (pH = 4)] on the diameter of semiconducting SWNTs measured under 10 mM KCl solution.

Figure 7 shows the diameter dependence of the threshold voltage shift due to pH. The threshold voltage shift is taken to be the difference between pH 10 and pH 4. While the very large diameters may be individual bundles, there is a clear trend for a larger shift for smaller diameter semiconducting SWNTs. This trend is in contrast to the expectation for direct charge-transfer processes that are chirality-dependent[28] where smaller band gap SWNTs can more easily accept or donate electrons. However, our pH and concentration dependence measurements indicate that the threshold voltage shift is not likely to be a direct charge-transfer process.

Our treatment of the pH-dependent electron-transport characteristics of SWNTs is admittedly oversimplified and, in the absence of experimentally determined surface charge densities, caution must be taken in quantifying these results. However, this simple treatment allows some intuitive insights into the pH-dependent electron-transport properties of SWNTs. One plausible picture arising from our measurements and the above considerations is the following. Under aqueous electrolyte solutions, SWNTs become charged due to possible surface chemical groups. These charges induce a potential offset in the gate voltage via a "field effect" which causes band bending in the SWNT leading to carrier injection from the metal contacts. The result of protonation (lowering the pH) is the removal of these surface charge effects which, experimentally, appear as a negative threshold voltage shift via hole removal (or electron injection). The larger threshold shift observed for smaller diameter SWNTs shown in Figure 7 may then be qualitatively rationalized by the fact that smaller diameter tubes with larger curvature tend to have higher reactivity and are therefore more likely to possess a larger number of chargeable surface functional groups.

Conclusions

We have shown that SWNT transistors exhibit significant pH-dependent electron-transport properties with negative shift of the threshold voltage with decreasing pH. Increasing the inert electrolyte concentration leads to screening of these pH-induced changes. No significant differences in the pH-dependent transport characteristics are found with various types of metal contacts. Based on the comparison with suspended SWNT transistors, pH-dependent charging of the substrate has been ruled out as the origin of the observed electrical response. The negative threshold voltage shift at low pHs indicates that, at least for electrically contacted semiconducting SWNTs, protonation does *not* lead to hole doping. In solution-dispersed SWNTs where hole doping upon protonation has been suggested, complications from surfactants, high shear mixing, and ultrasonication-induced damages and possible (partial) aggregation/bundling may lead to different behavior then what we observe here for the isolated bare SWNTs. One possible origin of the electrical response of SWNTs that is consistent with both concentration and pH dependencies may be the presence of surface-chargeable groups which give higher charge densities at high pHs. Such surface charges may explain the observed negative threshold voltage shift with decreasing pH as well as the larger response in smaller diameter semiconducting tubes. However, experimental verification of the nature and the quantity of such surface functional groups at the single nanotube level remains a challenge but will be especially important in developing applications that require SWNT−electrolyte interfaces.

Acknowledgment. This work was supported by the NSF (Grant Nos. CCF-0506660 and DMR-0348585). Part of the research for this publication was carried out in the Center for Microanalysis of Materials, University of Illinois at Urbana-Champaign, which is partially supported by the U.S. Department of Energy under Grant DEFG02-91-ER45439.

References and Notes

(1) (a) Yaish, Y.; Park, J. Y.; Rosenblatt, S.; Sazonova, V.; Brink, M.; McEuen, P. L. *Phys. Rev. Lett.* **2004**, *92*, 046401. (b) Javey, A.; Guo, J.; Wang, Q.; Lundstrom, M.; Dai, H. *Nature* **2003**, *424*, 654. (c) Yu, M.-F.; Files, B. S.; Arepalli, S.; Ruoff, R. S. *Phys. Rev. Lett.* **2000**, *84*, 5552.

(2) Sazonova, V.; Yaish, Y.; Ustunel, H.; Roundy, D.; Arias, T. A.; McEuen, P. L. *Nature* **2004**, *431*, 284−287.

(3) Cao, Q.; Zhu, Z. T.; Lemaitre, M. G.; Xia, M. G.; Shim, M.; Rogers, J. A. *Appl. Phys. Lett.* **2006**, *88*, 113511.

(4) (a) Chen, X.; Tam, U. C.; Czlapinski, J. L.; Lee, G. S.; Rabuka, D.; Zettl, A.; Bertozzi, C. R. *J. Am. Chem. Soc.* **2006**, *128*, 6292. (b) Chen, R. J.; Bangsaruntip, S.; Drouvalakis, K. A.; Kam, N. W. S.; Shim, M.; Li, Y. M.; Kim, W.; Utz, P. J.; Dai, H. J. *Proc. Natl. Acad. Sci.* **2003**, *100*, 4984−4989.

(5) (a) Wise, K. E.; Park, C.; Siochi, E. J.; Harrison, J. S. *Chem. Phys. Lett.* **2004**, *391*, 207. (b) Huxtable, S. T.; Cahill, D. G.; Shenogin, S.; Xue, L. P.; Ozisik, R.; Barone, P.; Usrey, M.; Strano, M. S.; Siddons, G.; Shim, M.; Keblinski, P. *Nat. Mater.* **2003**, *2*, 731. (c) Ajayan, P. M.; Stephan, O.; Colliex, C.; Trauth, D. *Science* **1994**, *265*, 1212.

(6) (a) Zhou, X.; Park, J.-Y.; Huang, S.; Liu, J.; McEuen, P. L. *Phys. Rev. Lett.* **2005**, *95*, 146805. (b) Durkop, T.; Getty, S. A.; Cobas, E.; Fuhrer, M. S. *Nano Lett.* **2004**, *4*, 35. (c) Yao, Z.; Kane, C. L.; Dekker, C. *Phys. Rev. Lett.* **2000**, *84*, 2941.

(7) Guo, X.; Small, J. P.; Klare, J. E.; Wang, Y.; Purewal, M.; Tam, I.; Hong, B. H.; Caldwell, R.; Huang, L.; O'Brien, S.; Yan, J.; Breslow, R.; Wind, S. J.; Hone, J.; Kim, P.; Nuckolls, C. *Science* **2006**, *311*, 356.

(8) (a) Shim, M.; Back, J. H.; Ozel, T.; Kwon, K.-W. *Phys. Rev. B* **2005**, *71*, 205411. (b) Shim, M.; Siddons, G. P. *Appl. Phys. Lett.* **2003**, *83*, 3564. (c) Park, J.; McEuen, P. L. *Appl. Phys. Lett.* **2001**, *79*, 1363. (d) Heinze, S.; Tersoff, J.; Martel, R.; Derycke, V.; Appenzeller, J.; Avouris, Ph. *Phys. Rev. Lett.* **2002**, *89*, 6801. (e) Sumanasekera, G. U.; Adu, C. K. W.; Fang, S.; Eklund, P. C. *Phys. Rev. Lett.* **2000**, *85*, 1096. (f) Collins, P. G.; Bradley, K.; Ishigami, M.; Zettl, A. *Science* **2001**, *287*, 1801.

(9) Ramesh, S.; Ericson, L. M.; Davis, V. A.; Saini, R. K.; Kittrell, C.; Pasquali, M.; Billups, W. E.; Adams, W. W.; Hauge, R. H.; Smalley, R. E. *J. Phys. Chem. B* **2004**, *108*, 8794.

(10) (a) Engtrakul, C.; Davis, M. F.; Gennett, T.; Dillon, A. C.; Jones, K. M.; Heben, M. J. *J. Am. Chem. Soc.* **2005**, *127*, 17548. (b) Zhou, W.; Heiney, P. A.; Fan, H.; Smalley, R. E.; Fischer, J. E. *J. Am. Chem. Soc.* **2005**, *127*, 1640.

(11) Zhao, W.; Song, C. H.; Pehrsson, P. E. *J. Am. Chem. Soc.* **2002**, *124*, 12418.

(12) O'Connell, M. J.; Bachilo, S. M.; Huffman, C. B.; Moore, V. C.; Strano, M. S.; Haroz, E. H.; Rialon, K. L.; Boul, P. J.; Noon, W. H.; Kittrell, C.; Ma, J. P.; Hauge, R. H.; Weisman, R. B.; Smalley, R. E. *Science* **2002**, *297*, 593.

(13) Strano, M. S.; Huffman, C. B.; Moore, V. C.; O'Connell, M. J.; Haroz, E. H.; Hubbard, J.; Miller, M.; Rialon, K.; Kittrell, C.; Ramesh, S.; Hauge, R. H.; Smalley, R. E. *J. Phys. Chem. B* **2003**, *107*, 6979.

(14) Weisman, R. B.; Bachilo, S. M.; Tsyboulski, D. *Appl. Phys. A* **2004**, *78*, 1111.

(15) Dukovic, G.; White, B. E.; Zhou, Z. Y.; Wang, F.; Jockusch, S.; Steigerwald, M. L.; Heinz, T. F.; Friesner, R. A.; Turro, N. J.; Brus, L. E., *J. Am. Chem. Soc.* **2004**, *126*, 15269.

(16) (a) Rosenblatt, S.; Yaish, Y.; Park, J.; Gore, J.; Sazonova, V.; McEuen, P. L. *Nano Lett.* **2002**, *2*, 869. (b) Krüger, M.; Buitelaar, M. R.; Nussbaumer, T.; Schönenberger, C.; Forró, L. *Appl. Phys. Lett.* **2001**, *78*, 1291.

(17) Kong, J.; Soh, H. T.; Cassell, A. M.; Quate, C. F.; Dai, H. *Nature (London)* **1998**, *395*, 878.

(18) Wang, C.; Cao, Q.; Ozel, T.; Gaur, A.; Rogers, J. A.; Shim, M. *J. Am. Chem. Soc.* **2005**, *127*, 11460.

(19) Shim, M.; Ozel, T.; Gaur, A.; Wang, C. *J. Am. Chem. Soc.* **2006**, *128*, 7522.

(20) Hu, H.; Yu, A. P.; Kim, E.; Zhao, B.; Itkis, M. E.; Bekyarova, E.; Haddon, R. C. *J. Phys. Chem. B* **2005**, *109*, 11520.

(21) Kim, U. J.; Furtado, C. A.; Liu, X. M.; Chen, G. G.; Eklund, P. C. *J. Am. Chem. Soc.* **2005**, *127*, 15437.

(22) Kim, W.; Javey, A.; Vermesh, O.; Wang, Q.; Li, Y.; Dai, H. *Nano Lett.* **2003**, *3*, 193.

(23) (a) Claye, A.; Rahman, S.; Fischer, J. E.; Sirenko, A.; Sumanasekera, G. U.; Eklund, P. C. *Chem. Phys. Lett.* **2001**, *333*, 16. (b) Rao, A. M.; Eklund, P. C.; Bandow, S.; Thess, A.; Smalley, R. E. *Nature (London)* **1997**, *388*, 257.

(24) (a) Chen, G.; Furtado, C. A.; Kim, U. J.; Eklund, P. C. *Phys. Rev. B* **2005**, *72*, 155406. (b) Chen, G.; Furtado, C. A.; Bandow, S.; Iilima, S.; Eklund, P. C. *Phys. Rev. B* **2005**, *71*, 045408.

(25) Szekeres, M.; Dekany, I.; de Keizer, A. *Colloids Surf., A* **1998**, *141*, 327.

(26) Shimotani, H.; Kanbara, T.; Iwasa, Y.; Tsukagoshi, K.; Aoyagi, Y.; Kataura, H. *Appl. Phys. Lett.* **2006**, *88*, 073104.

(27) Umpleby, R. J.; Baxter, S. C.; Chen, Y. Z.; Shah, R. N.; Shimizu, K. D. *Anal. Chem.* **2001**, *73*, 4584.

(28) O'Connell, M. J.; Eibergen, E. E.; Doorn, S. K. *Nat. Mater.* **2005**, *4*, 412.